

# Dynamics of the Chirped Return-to-Zero Modulation Format

R.-M. Mu, T. Yu, V. S. Grigoryan, and C. R. Menyuk, *Fellow, IEEE, Fellow, OSA*

**Abstract**—We numerically simulated long-distance, high-bit-rate, wavelength division multiplexed (WDM) transmission in dispersion-managed systems. We investigated return-to-zero (RZ) and nonreturn-to-zero (NRZ) modulation formats with amplitude and phase modulation. Consistent with earlier experiments, we find that the chirped return-to-zero (CRZ) modulation format has significant advantages over the NRZ modulation format in WDM systems. We elucidate the physical reasons for these advantages. We then discuss, in detail, the dynamics of the CRZ systems, carefully distinguishing noise effects, single-channel nonlinear effects, and multichannel nonlinear effects. In this way, we provide a physical basis for understanding CRZ systems that should prove useful for future system design. In particular, we find that the pulse evolution is dominated by linear dispersion and that the spread in the eye diagrams is dominated by signal-spontaneous beat noise, just like in linear systems. However, we also find that symmetric dispersion compensation performs better than asymmetric dispersion compensation, due to the effects of nonlinearity. Additionally, we find that interchannel nonlinearities spread the eye diagrams without changing the dynamical behavior. Thus, the system is quasilinear in the sense that its properties resemble those of linear systems, but nonlinearity plays an important role.

**Index Terms**—Amplified spontaneous emission (ASE) noise, chirped return-to-zero (RZ), nonlinearity, quasilinear, slope compensation, symmetric, wavelength division multiplexing (WDM).

## I. INTRODUCTION

**H**ISTORICALLY, optical communications systems used the nonreturn-to-zero (NRZ) modulation format for transmitting information. This modulation format was easier to generate than the return-to-zero (RZ) modulation format and has a smaller bandwidth per bit. However, the advent of long-haul wavelength division multiplexed (WDM) systems operating at distances greater than 5000 km and individual channel bit rates of 10 Gb/s has made it essential to effectively mitigate the nonlinearities and other impairments that accumulated during the transmission [1]. Recent experiments have

indicated that an RZ modulation format with an initial chirp (CRZ) performs better than the traditional NRZ modulation format [2]–[4]. In this paper, we present a series of simulations whose purpose is to compare NRZ, RZ, and CRZ systems, and then to systematically study the dynamics of the CRZ systems. The goal is to better understand the evolution of CRZ pulses and to carefully distinguish the impact of amplified spontaneous emission (ASE) noise, single-channel nonlinear effects, and multichannel nonlinear effects. Thus, we provide a physical basis for understanding CRZ systems that should prove useful in system design.

We begin our investigation by examining the power margins for the NRZ, RZ, and CRZ modulation formats in Section II at several map lengths in which it is possible to achieve an error-free transmission distance up of 10 000 km. We find that the lowest power level, which is set by ASE noise, is nearly the same for all three modulation formats. By contrast, the upper level, which is set by single-channel nonlinearity, is substantially higher for the CRZ modulation format than the other two modulation formats at any given distance. In Section III, we discuss the evolution of a single CRZ pulse in a channel that is several nanometers away from the zero-dispersion point. We find that the pulse duration stretches and shrinks by many times its initial amount as it passes through each period of the dispersion map. This stretch is far larger than a traditional periodically stationary dispersion managed soliton (DMS) system can tolerate [5], [6]. We also find that the initial chirp and the overall dispersion in the line must balance in order for the pulse to reach a minimum pulse duration at the end of the transmission line. Dispersion compensation at the beginning, at the end, or at both ends of the transmission line is required because of the dispersion slope. The final pulse duration is about a factor of two *smaller* than the initial pulse duration for practical values of chirp. The balance between initial chirp, overall dispersion, and the final pulse duration is accurately calculated when nonlinear effects are ignored, indicating that the nonlinear contribution to the pulse evolution is small. Moreover, we find that a Gaussian pulse approximation yields useful analytical estimates for the relationship between initial chirp, overall dispersion, and the final pulse duration. In Section IV, we discuss the evolution of a train of CRZ pulses in a single channel. We find that the noise accumulation is dominated by signal-spontaneous beat noise, just as would be the case in a linear system. At the same time, we also find that symmetric dispersion compensation yields more open eyes than does asymmetric compensation. We explain the physical origin of this difference as a consequence of the system nonlinearity. Finally, we consider full WDM simulations in Section V. We observe that the nonlinear interchannel interactions

Manuscript received March 23, 2001; revised October 18, 2001.

R.-M. Mu was with the Department of Computer Science and Electrical Engineering, University of Maryland Baltimore County, Baltimore, MD 21250 USA. She is now with Tycom Laboratory, Eatontown, NJ 07724 USA.

T. Yu was with the Department of Computer Science and Electrical Engineering, University of Maryland Baltimore County, Baltimore, MD 21250 USA. He is now with Nortel Networks, Boca Raton, FL 33487 USA.

V. S. Grigoryan was with the Department of Computer Science and Electrical Engineering, University of Maryland Baltimore County, Baltimore, MD 21250 USA. He is now with CeLight Corporation, Silver Spring, MD 20904 USA.

C. R. Menyuk is with the Department of Computer Science and Electrical Engineering, University of Maryland Baltimore County, Baltimore, MD 21250 USA and also with PhotonEx Corporation, Maynard, MA 01754 USA.

Publisher Item Identifier S 0733-8724(02)00376-6.

increase the spread of the eye diagrams, limiting our ability to decrease channel spacings. Nonetheless, the interchannel non-linearity does not change the basic dynamic behaviors of the pulses that is essentially linear.

Section VI contains our conclusions. We find that the CRZ system is quasilinear in that the single-pulse evolution and the noise accumulation behave as one would expect in a linear system. At the same time, the nonlinearity plays an important role in designing the overall dispersion map and the channel spacings.

Our studies of this system are based on a variant of the nonlinear Schrödinger equation that we may write in the form [7]

$$\begin{aligned} i \frac{\partial U(z, t)}{\partial z} - \frac{1}{2} \beta''(z) \frac{\partial^2 U(z, t)}{\partial t^2} \\ - \frac{i}{6} \beta'''(z) \frac{\partial^3 U(z, t)}{\partial t^3} + \gamma |U(z, t)|^2 U(z, t) \\ = i\alpha(z)U(z, t) + \hat{F}(z, t). \end{aligned} \quad (1)$$

The quantity  $U(z, t)$  is the complex wave envelope,  $z$  and  $t$  are distance along the fiber and retarded time,  $\beta''(z)$  and  $\beta'''(z)$  are the second- and third-order dispersions, respectively,  $\gamma$  is the nonlinear coefficient, and  $\alpha(z)$  is the gain-loss coefficient. The quantity  $\hat{F}(z, t)$  is the contribution of the ASE noise. We may write  $\gamma = n_2 \omega_0 / A_{\text{eff}} c$ , where  $n_2 = 2.6 \times 10^{-16} \text{ cm}^2/\text{W}$  is the Kerr coefficient,  $\omega_0$  is the central radial frequency of the light,  $c$  is the speed of light, and  $A_{\text{eff}}$  is the effective area of the fiber. For most of our simulations, we chose  $A_{\text{eff}} = 50 \mu\text{m}^2$ , which is a typical value for standard fiber, but for some of our simulations in Section V, we chose  $A_{\text{eff}} = 85 \mu\text{m}^2$ , corresponding to large effective area fiber (LEAF). We assume a fiber loss of 0.21 dB/km, and we assume that gain in the amplifiers balances the loss, so that we do not take into account gain saturation. The Langevin coefficient  $\hat{F}(z, t)$  is defined by its autocorrelation function

$$\langle \hat{F}(z, t) \hat{F}^*(z', t') \rangle = 2\theta(z)G(z)\hbar\omega_0\delta(z - z')\delta(t - t') \quad (2)$$

where spontaneous emission factor  $\theta(z) = n_{\text{sp}}$  at an amplifier and is zero elsewhere,  $G(z)$  is the amplifier gain, and  $\hbar$  is the Planck's constant. We solve (1) using the split-step method. Our approach is standard and was described in [7].

We are using the following approach to evaluate the performance of the systems. From our calculated eye diagrams, which include the effect of a square-law-detector and a fifth-order electrical Bessel filter with an 8-GHz full-width at half-maximum (FWHM) bandwidth, we calculate the signal-to-noise ratio (SNR)

$$\text{SNR} = \frac{I_1}{I_0} \quad (3)$$

where  $I_1$  is the average received current for the marks and  $I_0$  is the average received current for the spaces. In our simulations, we typically use 64 bits in each channel and six runs with different ASE noise realizations. We have verified that the SNR is a stable measure of the performance when we increase the bit string or the number of realizations. From the SNR, we can es-

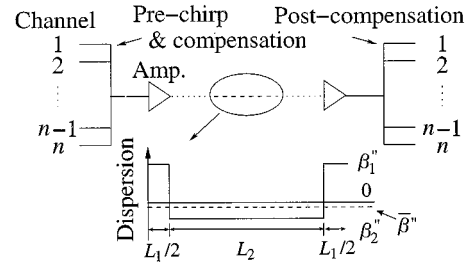


Fig. 1. Schematic illustration of the WDM transmission system used by Bergano *et al.* [2], [4].

timate the bit error rate (BER) using the formula [8]

$$Q = \frac{I_1 - I_0}{\sigma_1 + \sigma_0} \approx \frac{\text{SNR}}{\sqrt{(2\text{SNR} + 1) + 1}} \sqrt{\frac{B_o}{B_e}}, \quad (4)$$

$$\text{BER} \approx \frac{1}{\sqrt{2\pi} Q} \exp\left(\frac{-Q^2}{2}\right) \quad (5)$$

where  $B_o$  is the bandwidth of the optical filter in the system and  $B_e$  is the bandwidth of the electrical filter at the receiver. The estimates in (4) and (5) are not expected to be accurate because they are based on the assumption that both the marks and spaces are Gaussian-distributed noise; it is known that their distribution is more complex [8]. However, these estimates do provide a useful measure of system performance.

## II. COMPARISON OF RZ AND NRZ MODULATION FORMATS

To begin our studies, we consider a dispersion map that consists of two equal spans of fiber with alternating signs of the dispersion. We chose  $D_1 = -2.0 \text{ ps/nm-km}$  and  $D_2 = 2.0 \text{ ps/nm-km}$ , corresponding to  $\beta_1'' = 2.54 \text{ ps}^2/\text{km}$  and  $\beta_2'' = -2.54 \text{ ps}^2/\text{km}$ . Although these alternating dispersion values are not currently realistic, we have found that as long as the dispersion management strength parameter [5]

$$\gamma = 2 [(\beta_1'' - \bar{\beta}'') L_1 - (\beta_2'' - \bar{\beta}'') L_2] / \tau_{\text{FWHM}}^2 \quad (6)$$

remains constant, where  $L_1$  and  $L_2$  are the lengths of the two spans of the dispersion map, and  $\tau_{\text{FWHM}}$  is the FWHM pulse duration, then the behavior does not change much in the systems that we studied. The total propagation distance was 10 000 km, and we studied maps with periods of 100, 200, 500, 1000, 2000, and 10 000 km. The amplifier spacing is 50 km. There is no filter in the transmission line. The other parameters are the same as described in Section I. The structure of the WDM system is shown in Fig. 1.

Phase modulation and amplitude modulation may be used to decrease nonlinearly induced intersymbol interference [9]–[16]. The prechirp technique is relatively easy to use because it is only necessary to add a lithium-niobate phase modulator after the amplitude modulator. If a directly modulated signal is transmitted, it is only necessary to add a sinusoidal modulation current to the laser diode [9]. Assuming that the phase modulation  $\phi$  and the amplitude modulation  $U$  are bit synchronized, we may write

$$\phi = A\pi \cos(\Omega t), \quad (7a)$$

$$U = \frac{1}{2} U_0 (1 + \cos \Omega t) \quad (7b)$$

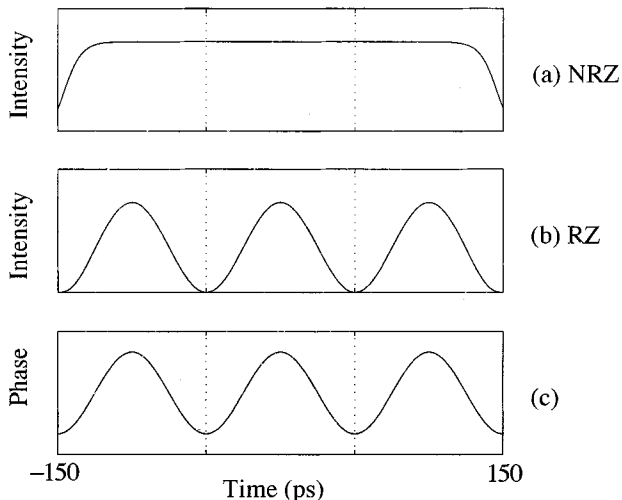


Fig. 2. Modulation formats and the corresponding bit-synchronized phase modulation for the bit string “111.” (a) NRZ intensity modulation. (b) RZ intensity modulation. (c) Phase modulation for both amplitude modulation formats.

where  $A$  is the modulation depth,  $\Omega/2\pi$  is the bit rate of the signal,  $t$  is time, and  $U_0$  is the initial pulse amplitude. Fig. 2 shows the bit-synchronized phase modulation for both the NRZ and RZ modulation formats with the bit string “111.” The variation of the phase modulation is very similar to the variation of the amplitude modulation of the RZ format.

We first investigated the power margin for each of the dispersion-map periods. We define the power margins as the power range in which  $Q > 6$ , corresponding to a BER  $\lesssim 10^{-9}$ , where we have used the definitions in (4) and (5). In Fig. 3, we show our results. Fig. 3(a) shows the margins when there is no phase modulation on the initial pulse trains, and Fig. 3(b) shows the results when there is phase modulation. Two salient points emerge. First, the power margins are consistently better with RZ than they are with NRZ. Second, phase modulation improves performance. We investigated a range of chirp parameters,  $0.2 < |A| < 1$ , where  $A$  is defined as in (7a), and we found that over this range, the improvement was roughly the same. Beyond the value  $|A| = 1$ , the signal bandwidth becomes unacceptably large for WDM applications.

A number of physical phenomena are occurring that lead to these results. First, we note that the lower power level at which the system performance becomes unacceptable is almost independent of whether RZ or NRZ is used, whether the pulses are chirped or unchirped, or the length of the dispersion map. In all cases, it is approximately 0.3 mW. By contrast, the upper levels depend sensitively on these choices; thus, we conclude that a correct choice of these parameters allows us to manage the nonlinearity successfully. Second, receiver sensitivity to RZ pulses is several decibels better than it is for NRZ when passed through standard receivers. We found, during our investigation, that when the RZ pulses are appropriately chirped, they compress over the propagation distance, which increases this advantage. This compression occurs in a quasilinear fashion that has a simple analytical description, as we will discuss in the next section. A similar quasilinear behavior has been observed pre-

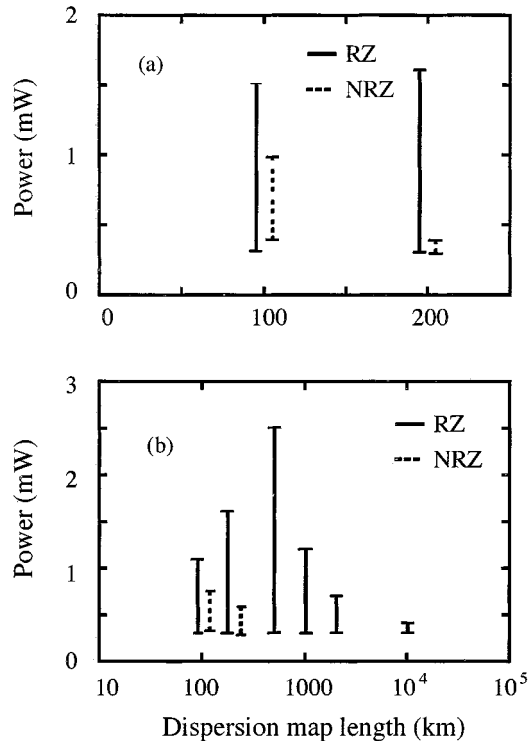


Fig. 3. Power margin of the output signal (a) without phase modulation and (b) with phase modulation, setting  $A = 0.5$ .

viously by Georges *et al.* [17], although the system parameters are quite different.

Given the clearly superior power margins that RZ signals have relative to NRZ signals, we focused the remainder of our studies on RZ signals.

### III. DYNAMICS OF SINGLE-CHANNEL RZ PULSE PROPAGATION

#### A. Pulse Compression

Next, we focus on single-channel RZ propagation in order to better understand the RZ signal evolution. We describe a case in which the average dispersion in the transmission line differs significantly from zero, which is the case for most channels in a WDM system, and allows us to discuss the dynamics of dispersion compensation. The dispersion map that we used for this study has one segment of length  $L_1 = 160$  km with  $D_1 = -2.125$  ps/nm-km and a second segment of length  $L_2 = 20$  km with  $D_2 = 17.0$  ps/nm-km at  $1.55 \mu\text{m}$ , corresponding to the point at which the average dispersion is zero. We assume a dispersion slope  $dD/d\lambda = 0.075$  ps/nm<sup>2</sup>-km, and we assume that the channel is displaced  $-4.8$  nm from the point of zero average dispersion. After the appropriate conversions, we find that  $\beta_1'' = 3.128$  ps<sup>2</sup>/km, corresponding to  $D_1 = -2.44$  ps/nm-km, and we find that  $\beta_2'' = -21.22$  ps<sup>2</sup>/km, corresponding to  $D_2 = 16.55$  ps/nm-km. Hence, the average dispersion of each dispersion map  $\bar{\beta}''$  equals  $0.423$  ps<sup>2</sup>/km, corresponding to  $\bar{D} = -0.33$  ps/nm-km. The amplifier spacing is 45 km, and the total propagation distance is 5040 km. These parameters correspond to the experiments of Bergano *et al.* [2], [4], except that our  $A_{\text{eff}}$  is smaller, and our dispersion map period is smaller. We chose it

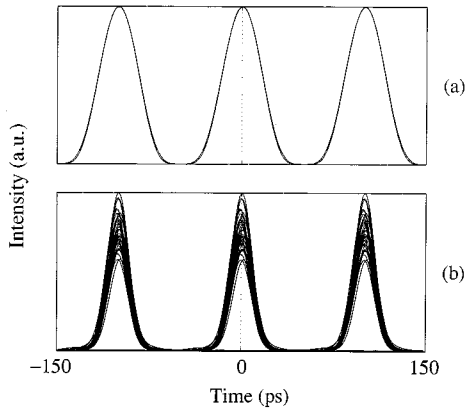


Fig. 4. Eye diagrams in the optical domain of (a) the input and (b) the output for the chirped RZ pulse when the average dispersion is undercompensated.

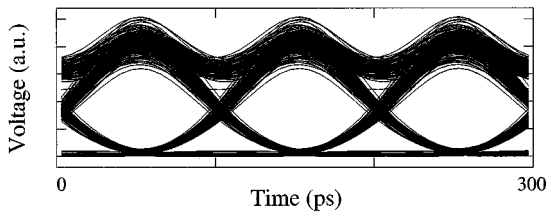


Fig. 5. Output eye diagram in the electrical domain under the same conditions as in Fig. 4.

so that the dispersion management strength parameter  $\gamma$  corresponds to the value at which our studies in Section II showed the largest margin. We verified that this value also corresponds to nearly the largest eye opening once other parameters like the dispersion compensation are optimized. For our simulations in this section, we chose a phase modulation depth  $A = -0.6$ , which our previous studies indicated was within the optimal range, and an average power of 0.5 mW at the input, which, again, yielded nearly the largest eye openings.

Fig. 4 shows the optical eye diagrams for an optimized case. We use this case as a baseline to study the effects of parameter variations. We calculate the optical eye diagrams by superposing the optical power for all the bits in our simulation. For the case shown here, we compensate for the dispersion symmetrically. In other words, we add equal amounts of compensation at the beginning and at the end of the link. We will show later in this section that this choice is better than using just precompensation or just postcompensation. After the dispersion compensation, the overall average dispersion of the whole transmission line  $\delta\bar{D}$  equals  $-0.025$  ps/nm-km ( $\delta\bar{\beta}'' = 0.0321$  ps<sup>2</sup>/km). Thus, the line is undercompensated, which our simulations show yields optimal results. Later in this section, we present a theory that allows us to explain the desirability of under- or overcompensation and to calculate its approximate magnitude. The dispersion parameters that we chose here correspond to a typical case in a WDM system that requires dispersion compensation. Fig. 5 shows the electrical eye diagrams at the receiver.

A salient point that emerges from examination of Figs. 4 and 5 is that the principal contribution of the ASE noise from the amplifiers is to the amplitude jitter of the marks, also referred to as signal-spontaneous beat noise. In this respect, the system resembles standard NRZ systems far more than standard soliton

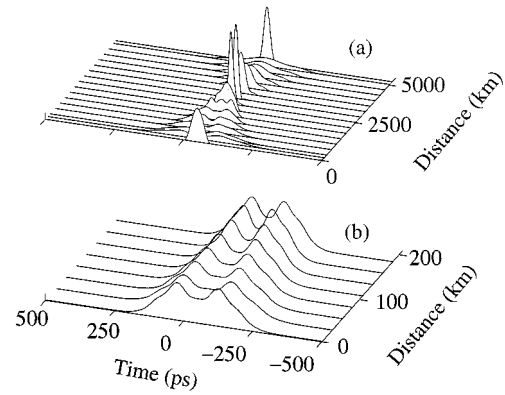


Fig. 6. Evolution of the chirped RZ pulse (a) along the entire propagation length and (b) inside the third dispersion map.

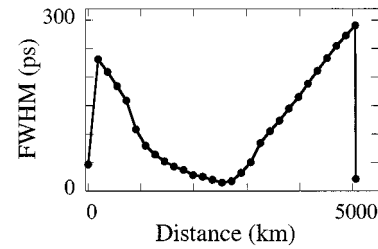


Fig. 7. Evolution of the pulse duration at the end of each map period.

systems that are typically dominated by timing jitter [18], [19] or filtered dispersion-managed soliton systems that are dominated by the growth of noise in the spaces [20].

A second salient point that emerges from examination of Fig. 4 is that at the end of the transmission, the pulse duration has compressed so that it is slightly smaller than half the original amount. This compression occurs after a complex evolution, as shown in Fig. 6. In Fig. 6(a), we show the evolution of a single CRZ pulse after every 360 km, which is twice the dispersion map period. The first and the last pulse shape correspond to the CRZ pulse before and after the dispersion slope compensation. This single chirped pulse first stretches after the initial slope compensation by a factor of about five or six times its initial duration. During the propagation, the opposite sign of the residual dispersion in the transmission fiber, combined with the pulse chirp, leads to a gradual pulse compression until the pulse reaches its minimum duration at the midpoint of the propagation. Then, the pulse stretches out again until it resumes a pulse duration of five or six times the original amount before the final compensation. After the final compensation, the pulse is, once again, narrow. In Fig. 6(b), we show the evolution of the pulse shape during the third map period where the pulse is most stretched. We find that the maximum pulse duration is only a factor of 1.2 larger than the minimum duration inside this dispersion-map period. In general, the ratio of the maximum to the minimum pulse duration in each dispersion map is never larger than a factor of two or three. In Fig. 7, we summarize the evolution by showing the pulse duration at the end of each map period.

This evolution differs significantly from the evolution of periodically stationary dispersion-managed solitons. Their maximum stretching factors must be less than a factor of about

three to avoid large nonlinear impairments [5], [6]. The large stretching factor in the CRZ system reduces the effect of non-linearity.

### B. Gaussian Linear Theory

We may better understand the behavior seen in Fig. 4 by comparison to linear pulse propagation of a Gaussian-shaped pulse. First, we expand the bit-synchronized phase modulation using a Taylor series as

$$A\pi \cos(\Omega t) = A\pi \left(1 - \frac{1}{2}\Omega^2 t^2 + \frac{1}{24}\Omega^4 t^4 - \dots\right). \quad (8)$$

The first term on the right-hand side of the equation corresponds to a constant phase shift, the second term corresponds to a quadratic phase term that leads to a linear chirp, and the rest corresponds to higher order terms. An initial chirped Gaussian pulse at  $z = 0$  may be written as

$$U(0, t) = \exp \left[ -\frac{(1 + ic_0)t^2}{2T_0^2} \right] \quad (9)$$

where  $U$  is the wave envelope, and  $T_0$  and  $c_0$  are the initial pulse duration and chirp coefficient. The approximate linear evolution of the pulse is governed by the equation

$$i \frac{\partial U(z, t)}{\partial z} - \frac{1}{2} \beta''(z) \frac{\partial^2 U(z, t)}{\partial t^2} = 0 \quad (10)$$

where  $\beta''(z)$  is the group velocity dispersion. The analytical solution for this Gaussian chirped pulse at distance  $z = Z$  may be written as [21]

$$U(Z, t) = \frac{T_0}{\left[ T_0^2 - i \int_0^Z \beta''(z)(1 + ic_0) dz \right]^{1/2}} \times \exp \left[ -\frac{(1 + ic_0)t^2}{2 \left[ T_0^2 - i \int_0^Z \beta''(z)(1 + ic_0) dz \right]} \right]. \quad (11)$$

Then the dependence of the pulse duration  $T_{\text{out}}$  on the total distance in the linear dispersive medium is

$$\frac{T_{\text{out}}}{T_0} = \left[ \left( 1 + \frac{c_0 \int_0^Z \beta''(z) dz}{T_0^2} \right)^2 + \left( \frac{\int_0^Z \beta''(z) dz}{T_0^2} \right)^2 \right]^{1/2}. \quad (12)$$

If we define the average dispersion  $\delta\bar{\beta}''$  from the relation  $\int_0^Z \beta''(z) dz = \delta\bar{\beta}'' Z$ , one can see that when  $\delta\bar{\beta}'' c_0 < 0$ , the pulse will initially compress. In this case, the minimal pulse duration occurs at the end of the propagation, and its value is given by

$$Z_{\text{min}} \delta\bar{\beta}'' = -\frac{c_0}{1 + c_0^2} T_0^2 \quad (13)$$

$$\frac{T_{\text{min}}}{T_0} = \frac{1}{(1 + c_0^2)^{1/2}}. \quad (14)$$

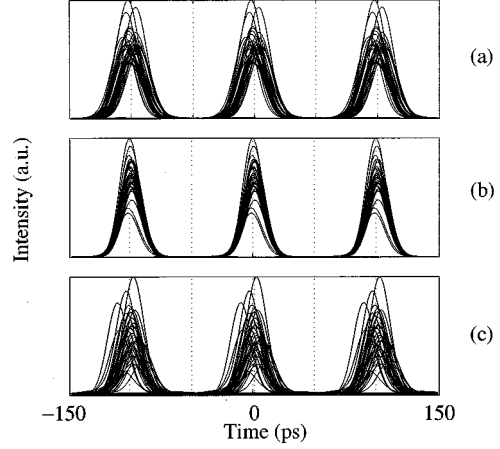


Fig. 8. Compression of the input pulse under different conditions. (a)  $A = -0.3$ ,  $CD = 86.1\%$ , (b)  $A = 0.6$ ,  $CD = 107.9\%$ , and (c)  $A = -0.3$ ,  $CD = 91.8\%$  with a transmission distance of 10 080 km. All other parameters are the same as in Fig. 4.

Comparing (8) and (9), we find that

$$c_0 = A\pi\Omega^2 T_0^2. \quad (15)$$

Now, we compare the predictions of this simple linear theory to the actual optimized evolution that we have already shown in Fig. 4. We recall that, for this system, the system parameters are  $A = -0.6$ , and  $\delta\bar{\beta}'' = 0.0321$  ps<sup>2</sup>/km ( $\delta\bar{D} = -0.025$  ps/nm-km). The quantity  $Z_{\text{min}}$  equals 5040 km, which is the total length. It is useful to characterize this kind of system using the compensation degree (CD)

$$CD = 1 - \frac{\delta\bar{\beta}''}{\beta''} \quad (16)$$

where  $\bar{\beta}''$  is the average dispersion over one dispersion map. Undercompensation corresponds to  $CD < 1$ , whereas overcompensation corresponds to  $CD > 1$ . In this case,  $CD = 92.7\%$ , so the system is undercompensated. We find, from Fig. 4, that  $T_{\text{out}}/T_0 = 0.31$ . However, (12)–(15) predict  $\delta\bar{\beta}'' = 0.027$  ps<sup>2</sup>/km ( $\delta\bar{D} = -0.021$  ps/nm-km), corresponding to  $CD = 93.6\%$  and  $T_{\text{out}}/T_0 = 0.133$ . Linearly, there is a discrepancy because the initial phase modulation is sinusoidal rather than quadratic and because the initial pulse shape is raised-cosine rather than Gaussian. There is also an additional discrepancy due to the nonlinearity. If we solve (10) using the actual pulse shape and keeping CD the same, so that the only discrepancy is due to the nonlinearity, then we find that  $T_{\text{out}}/T_0 = 0.29$ . Thus, the portion of the discrepancy that is due to the nonlinearity is relatively small.

### C. Parameter Variations

Now, we consider the effect on the evolution of varying the system parameters and examine the validity of (12)–(15).

In Fig. 8, we show output eye diagrams when we vary the phase modulation depth  $A$  and the system length. In Fig. 8(a), we increase the phase modulation depth from  $A = -0.6$  to  $A = -0.3$ , and in Fig. 8(b), we increase it again to  $A = 0.6$ . For the case shown in Fig. 8(a), the optimal compensation degree CD equals 86.1%, whereas, for the case shown in Fig. 8(b),

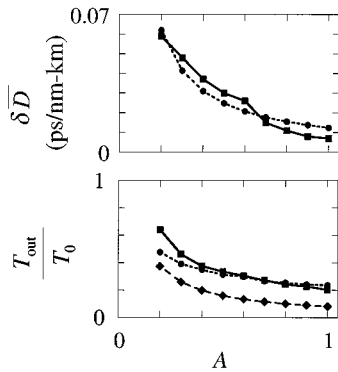


Fig. 9. Dependence on the modulation depth  $A$  of (a) the optimal dispersion and (b) the final pulse compression. The dotted line with squares is the result of complete simulations, while the solid line with circles is the result of neglecting nonlinearity. The dashed line in (b) is the result of Gaussian linear theory.

it equals 107.9%. By contrast, the values predicted by (12)–(15) are  $CD = 87.5\%$  in Fig. 8(a) and  $CD = 106.4\%$  in Fig. 8(b). Although these values differ somewhat from the actual values, the trends are correct. Similarly, we find that the values of  $T_{\text{out}}/T_0$  in Fig. 8(a) and (b) are 0.39 and 0.29, whereas the predicted values are 0.26 and 0.133. The deviations are larger for this parameter, but, again, we find that the trends are correct. Finally, in Fig. 8(c), we show the impact of doubling the system length to 10 080 km while other parameters are the same as in Fig. 4. It is clear that the optical eye diagram has deteriorated substantially. Because  $Z_{\text{min}}$  has increased by a factor of two,  $\delta\bar{\beta}''$  must decrease by approximately a factor of two, and, indeed, we find that  $CD = 91.8\%$ . The predicted value is  $CD = 93.7\%$ . The actual and predicted values of  $T_{\text{out}}/T_0$  are 0.40 and 0.26. Again, the trends are correct.

In Fig. 9, we show the actual values of  $\delta\bar{D}$  and  $T_{\text{out}}/T_0$  as a function of the phase modulation depth  $A$  when the pulses are optimally compressed at the end of the transmission. We also show the predictions of (12)–(15) and the predictions of linear theory. We find that the Gaussian approximation is qualitatively useful, but it is not quantitatively exact. However, when we use the modified linear theory, the predictions agree with the predictions of the complex nonlinear theory within 10% to 15%, indicating that the nonlinearity contributes little to the pulse evolution.

In order to verify our conclusion that the pulse evolution is dominated by the linear dispersion, with the nonlinearity only making a small contribution, we studied the pulse evolution for a wide variety of values of the initial modulation depth  $A$  and of the average dispersion in one period of the dispersion map  $\bar{\beta}''$ . We note that changes in  $\bar{\beta}''$  correspond to changes in the central wavelength. The evolution differs significantly, depending on our choice of parameters. For example, as  $|\bar{\beta}''|$  increases, corresponding to an increasing wavelength separation from the zero dispersion point, the maximum pulse expansion increases from approximately twice the pulse duration at a wavelength corresponding to the zero dispersion point to approximately five times the pulse duration at a wavelength corresponding to 4.8-nm separation from the zero dispersion point, assuming a net dispersion slope  $dD/d\lambda = 0.07$  ps/nm<sup>2</sup>-km, with the other parameters the same as in Fig. 4. Nonetheless,

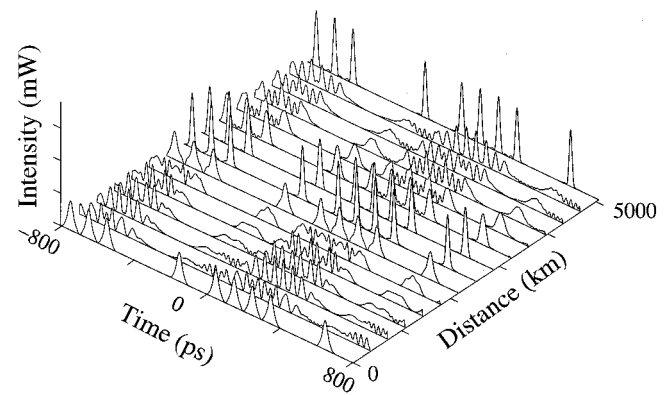


Fig. 10. Pulse interactions in a single channel with the same parameters as in Fig. 4, except without ASE noise and fiber loss.

the evolution is well described by the modified linear theory, as long as the signal average power is less than 1.0 mW, where we recall that the  $A_{\text{eff}} = 50$   $\mu\text{m}^2$ . At higher powers, nonlinearity substantially affects the pulse evolution, but, at the same time, the eye diagrams degrade significantly. Therefore, at the power levels associated with the experiments by Bergano *et al.* [2], [4], the pulse shape evolution is always close to linear.

#### IV. PATTERN DEPENDENCE AND AMPLITUDE JITTER

##### A. Pulse Interactions

In Fig. 6(a), we showed a single CRZ pulse propagating in a transmission system. The stretching factor of the pulse was large enough to lead to a significant overlap with its neighbors. Hence, one must ask how the nonlinear pulse interactions will affect the pulse dynamics. In dispersion-managed soliton systems, the pulse interactions are periodic, and significant interactions ultimately destroy the pulses [5]. Using a pseudorandom bit sequence of 64 bits and the same parameters, as in Fig. 6(a), we show the evolution of CRZ interactions in a single channel in Fig. 10. The pulses stretch by a factor of five to six times their original pulse durations, just as in the single pulse propagation, shown in Fig. 6. However, they could be recompressed without difficulty. Indeed, we find that their evolution is little affected by the nonlinear pulse interactions. We did not include ASE noise in this figure, but when we include it, the behavior is unchanged. The low nonlinearity limits the interpulse interference because, during most of the transmission line, the pulse trains act as a CW wave. As in the transmission of a single pulse, the pulses achieve their first minimum pulse durations in the center of the transmission. At the end of the propagation, the pulse durations are once again smaller. At intermediate points except the center, it is almost impossible to distinguish the marks from the spaces due to overlap of adjacent pulses. Nonetheless, the pulse stretching is not large enough for the nonlinear pulse interactions in a single channel to be attributed only to intrachannel four-wave mixing, and we see no evidence of ghost-pulse formation [22], [23].

##### B. Amplitude Jitter

The evolution of the CRZ pulses has a pattern dependence, as shown in Fig. 11. From the figure, one sees that the behavior of two consecutive marks “11” is different from “01.” A long

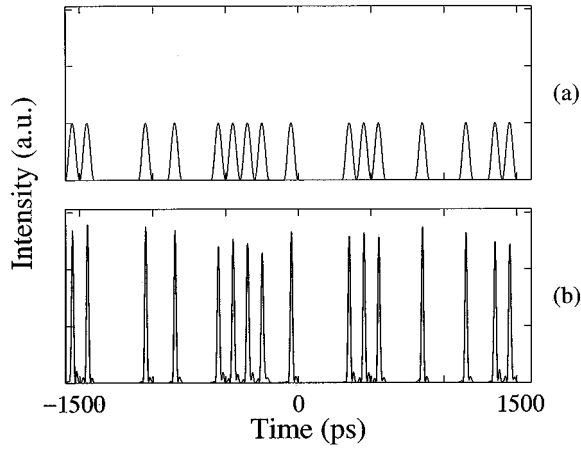


Fig. 11. Pattern dependence of the chirped RZ pulse. (a) Input signal. (b) Output signal with the same parameters as in Fig. 4.

sequence of marks evolves differently from a short sequence of marks. A pattern in which a mark is followed by a sequence of spaces will have a better SNR than a mark that is followed by other marks. This behavior is a consequence of interpulse interference in the transmission system due to the large stretching factor of the CRZ pulses. Adjacent pulses significantly overlap each other. ASE noise and the small nonlinearity combine to cause pulse interaction and energy exchange. Thus, the output of the CRZ modulation format is highly pattern dependent. By contrast, other NRZ or RZ modulation formats in which the pulses are not strongly stretched suffer from much less pattern dependence because the pulses do not overlap as dramatically as they do in CRZ systems.

As noted previously, the amplitude jitter of the marks is much larger than that of the spaces. To investigate the origin of the amplitude jitter, we tested the contribution of ASE noise, nonlinearity, and dispersion compensation to the jitter. In this set of simulations, we used  $1.5452 \mu\text{m}$  as the wavelength of the channel, and, like in Fig. 4, the results are obtained for a map with an average dispersion of  $\overline{D} = -0.33 \text{ ps/nm-km}$  ( $\overline{\beta}'' = 0.423 \text{ ps}^2/\text{km}$ ). We sequentially turn off the ASE noise and the nonlinearity, and vary the dispersion compensation. We obtain the results shown Fig. 12. Fig. 12(a) shows the eye diagram with nonlinearity and the same undercompensation as in Fig. 4 [ $\delta\overline{D} = -0.025 \text{ ps/nm-km}$  ( $\delta\overline{\beta}'' = 0.0321 \text{ ps}^2/\text{km}$ )], but without ASE noise. Fig. 12(b) shows the eye diagram with ASE noise and nonlinearity, but with complete compensation. Fig. 12(c) shows the eye diagram with ASE noise and the same undercompensation, but without nonlinearity. Fig. 12(d) shows the eye diagram without ASE noise or nonlinearity and with complete compensation. Comparing these figures with Fig. 4(b), where both ASE noise and the nonlinearity are taken into account and the dispersion is undercompensated, we note that ASE noise is the dominant factor that contributes to a large amplitude jitter of the marks. Fig. 12(a) shows that, without the ASE noise, the amplitude jitter of the marks is significantly reduced, implying that spontaneous-signal beat noise induces most of the amplitude jitter. Although nonlinearity and chromatic dispersion do contribute to the amplitude jitter as well as the timing jitter, these contributions can be made very small

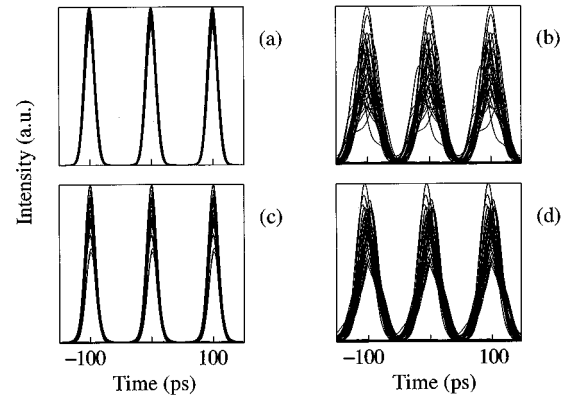


Fig. 12. Amplitude jitter of the chirped RZ pulse. (a) Eye diagram with nonlinearity and the same undercompensation as in Fig. 4 [ $\overline{D} = -0.025 \text{ ps/nm-km}$  ( $\overline{\beta}'' = 0.0321 \text{ ps}^2/\text{km}$ )], but without ASE noise. (b) Eye diagram with ASE noise and nonlinearity, but with complete compensation. (c) Eye diagram with ASE noise and the same undercompensation, but without nonlinearity. (d) Eye diagram without ASE noise or nonlinearity, and with complete compensation.

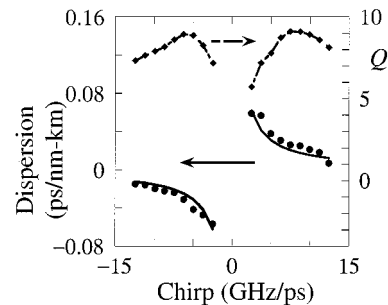


Fig. 13. Dependence on the modulation depth  $A$  of optimal path average dispersion and  $Q$ . The dashed lines with squares correspond to the  $Q$  values. Filled circles represent the optimal dispersion values calculated through numerical simulation, and solid lines are the optimal dispersion values calculated using Gaussian linear theory.

by appropriately choosing the overall dispersion and the initial chirp. In a transmission system based on the CRZ modulation format, it is important to diminish the effect of the ASE noise. One approach is to use LEAF fiber. Another is to use inline Raman amplification.

As we noted in Sections IV-A and IV-B, we can achieve optimal compression at the output by choosing  $\delta\overline{\beta}''$  correctly to match the initial chirp. Different initial chirps lead to different stretching factors of the pulses, but the qualitative behavior is the same in all cases, as long as  $\delta\overline{\beta}''$  is correctly chosen. The stretching factor can be reduced by decreasing the initial chirp, however; it is useful to achieve the largest possible stretching factor in order to maximally reduce the four-wave mixing and intersymbol interface. We have found that it is possible to maintain  $Q > 6$  for a modulation depth  $0.3 \leq |A| \leq 0.8$ , as shown in Fig. 13.

### C. Dispersion Compensation

Dispersion compensation is quite common in conventional NRZ transmission systems because the NRZ modulation format can only operate with nearly zero average dispersion over the whole transmission line. Dispersion compensation can be done by using dispersion-shifted fiber, optical gratings [24]–[26],

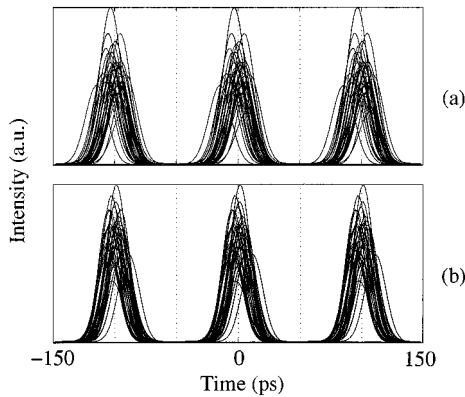


Fig. 14. Asymmetric dispersion compensation (a) before the transmission and (b) after the transmission. Compare this figure to Fig. 4.

or optical phase conjugation [27]. Dispersion compensation of the RZ modulation format is less important over a given length because the RZ modulation format is less degraded than the NRZ modulation format by nonlinearities. Nevertheless, as we previously showed, the CRZ modulation format operates best with dispersion compensation, and it is required to achieve the largest possible propagation length. For the central channel in the WDM system, the dispersion is periodically compensated and the average dispersion should be set close to zero. For the side channels, the transmission average dispersion  $\delta\bar{\beta}''$  was achieved by compensating the slope at the beginning and at the end of the transmission line. From a physical standpoint, it is possible to recompress the individual pulses at the end of the transmission because different overlapped pulses each have a different local frequency at the same point in time, so that they remain individually distinguishable. At each end, we compensated half of the net dispersion because, if we compensated the whole net dispersion only before or after the transmission, the results would be worse. In Fig. 14, we show the final eye diagrams when the dispersion compensation is done entirely before or entirely after the transmission. The parameters are the same as in Fig. 4. Comparing these results to symmetric compensation in Fig. 4, it is clear that symmetric compensation yields a better eye diagram than does asymmetric compensation. This result is in agreement with that of Ding *et al.* [16] and Hayee *et al.* [28]. They found that the accumulated dispersion and stretching factor with asymmetric compensation are larger than those with symmetric compensation. As discussed in Section III [Fig. 6(a)] and Section IV-A (Fig. 10), symmetric compensation cuts the transmission into two parts. This observation is important because it clearly indicates the important role that nonlinearity plays in these systems. Despite the nearly linear evolution of the CRZ pulses as they propagate along the fiber, and despite the domination of spontaneous-signal beat noise, which is one of the signatures of linear signal propagation, the system is definitely affected by nonlinearity. If the system was purely linear, it would not matter where the dispersion compensation occurred. We have studied the physical origin of this nonlinear effect. It occurs because when CRZ pulses overlap, their frequencies shift in just such a way that the pulses attract each other. This effect is well known in the theory of solitons [29]. The exact evolution

is somewhat complex in dispersion-managed systems like the ones that we are considering [30]. In brief, the sign of the time shift is determined by the sign of the product of the cumulative dispersion at the end of each map period times the frequency shift. When the compensation is symmetric, the cumulative dispersion changes sign midway through the propagation, so that the product of the cumulative dispersion times the frequency shift changes its sign. Hence, pulses that had previously attracted begin to repel. When the propagation has finished, the time shift returns nearly to zero. By contrast, when the compensation is asymmetric, the pulses always attract during the propagation because the sign of the product of the cumulative dispersion times the frequency shift is unchanged, leading to a large time shift. The magnitude of this time shift depends on the amplitude of the pulses, which in turn varies due to spontaneous-signal beat noise. Thus, this effect transforms amplitude jitter into timing jitter. The resulting timing jitter is clearly visible in Fig. 14.

Asymmetry due to the dispersion compensation in each map length, as well as the gain and loss variation along the transmission line, imply that the evolution is somewhat more complex than we just outlined. In practice, we find that the compensation at the beginning and at the end should be in approximately a 60 : 40 ratio for optimal performance.

## V. WDM STUDIES

There are many studies of WDM systems that focus on solitons, the NRZ modulation format, or the RZ modulation format. However, the performance of these systems is not acceptable at 10 Gb/s over transoceanic distances of 5000 km or more, or, in the case of some recent soliton experiments, the systems are currently considered by system engineers to be too complex to be built in practice. It was this observation that motivated Bergano *et al.* [2], [4] to introduce the CRZ modulation format. In this section, we will study the performance of the CRZ modulation format in WDM systems and the dependence of its performance on key parameters such as the dispersion slope and the effective area of the fiber core.

Kerr nonlinearity leads to interactions among WDM channels. It is desirable to suppress this interaction by properly adjusting the channel spacing and choosing the dispersion map. We study multichannel systems with seven or eight channels. Previous work [31] indicates that this number is sufficient to study the channel interactions in a full WDM system. Channels that are far away do not affect each other much because they pass through each other quickly, due to dispersion. In the WDM systems that we modeled, the channels are evenly spaced in wavelength, and each wavelength has a slightly different average dispersion. In all of our WDM simulations, we assumed that the EDFA has the same gain for all the WDM channels. In reality, the EDFAs may have a wavelength-dependent gain profile. Different channels will experience different gain. This effect can be extremely harmful in long-haul WDM systems. The accumulated gain difference must be avoided in practice by using passive, gain-equalizing filters [11], [32].

We consider systems with multiple channels using the CRZ modulation format. As in Fig. 4, we use the same dispersion

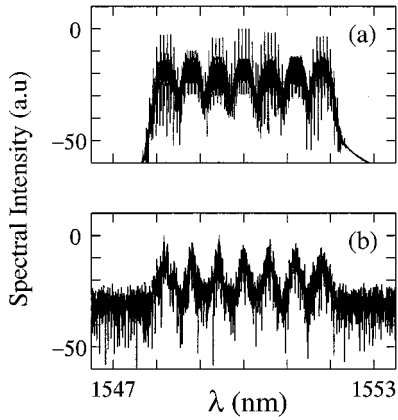


Fig. 15. Spectral intensity, plotted logarithmically, of the CRZ seven-channel system using standard fiber at the (a) input and the (b) output.

map as in Section III with the following parameters:  $D_1 = -2.125$  ps/nm-km ( $\beta_1'' = 2.724$  ps<sup>2</sup>/km);  $L_1 = 160$  km,  $D_2 = 17$  ps/nm-km ( $\beta_2'' = -21.795$  ps<sup>2</sup>/km); and  $L_2 = 20$  km at  $1.55$   $\mu$ m. The dispersion slope is  $0.075$  ps/nm<sup>2</sup>-km, and the total propagation distance is  $5040$  km. WDM systems are affected by intersymbol interference due to ASE noise and nonlinearity in a single channel. They are also affected by nonlinear interchannel interactions. In previous sections, we focused on single-channel intersymbol interference. Comparing the results of this section to those of the previous sections allows us to determine the importance of the interchannel interference. We noted in Section III-C that, as long as we keep the average dispersion over the entire transmission line  $\delta\beta''$  the same, we can obtain an optimally compressed pulse with a fixed chirp almost regardless of how the dispersion is distributed. In the WDM simulations that we describe here, we used the same average dispersion in every other channel, so that the chirp is the same in every other channel. In adjacent channels, we use the same magnitude of the chirp but with the opposite sign. Hence, the sign of  $\delta\beta''$  also changes. This choice is not critical, and the results are almost unchanged if we use a chirp with the same sign in each channel. We used a channel spacing of  $0.6$  nm, and we kept seven channels. The channel spacing is larger than in practical systems, but we do not use orthogonal polarizations in neighboring channels or forward error-correction coding, as in practical systems. Our goal is to study the additional impairments due to interchannel interactions.

The simulated results are shown in Figs. 15–17. The results are qualitatively the same as in the case of the single channel studies, but the channels are degraded. The eye diagrams are similar to the eye diagrams of the single-channel system, but with more amplitude jitter. As shown in Fig. 16, the pulses are all compressed at the end of the transmission, just as was the case with a single channel. Figs. 18–20 show the results using the same system parameters, except that we employ LEAF fibers. If we used this kind of fiber, the effective area changes from  $50$   $\mu$ m<sup>2</sup> to  $85$   $\mu$ m<sup>2</sup>, but the dispersion slope changes from  $0.075$  ps/nm<sup>2</sup>-km to  $0.1$  ps/nm<sup>2</sup>-km. We observed a significant reduction of the amplitude jitter, especially in the central channel, indicating that using LEAF fiber will benefit

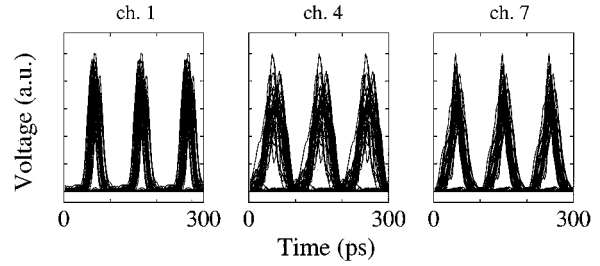


Fig. 16. Optical eye diagrams of the CRZ seven-channel WDM system using standard fiber. The eye opening is smaller than in a single channel system with the same system parameters.

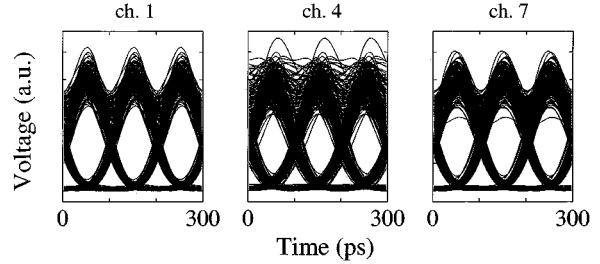


Fig. 17. Electrical eye diagrams of the CRZ seven-channel WDM system using standard fiber.

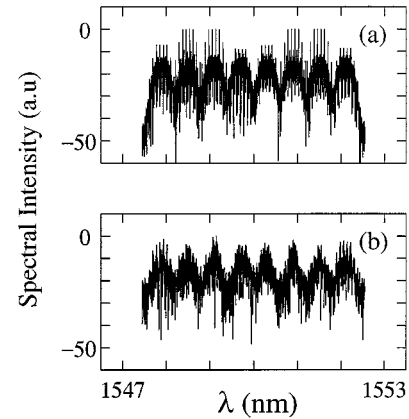


Fig. 18. Spectral intensity, plotted logarithmically, of the CRZ eight-channel system using LEAF fiber at the (a) input and the (b) output.

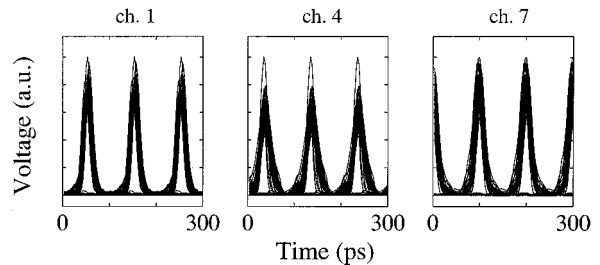


Fig. 19. Optical eye diagrams of the CRZ eight-channel WDM system using LEAF fiber. The eye opening is better than with standard fiber, especially the central channel.

the system performance, because the larger core area reduces the effect of nonlinearity.

From these simulations and others that we have made, we conclude that the interchannel interactions degrade the eye diagrams of the individual channels, but they do not greatly affect the pulse dynamics. The pulse evolution in each channel is

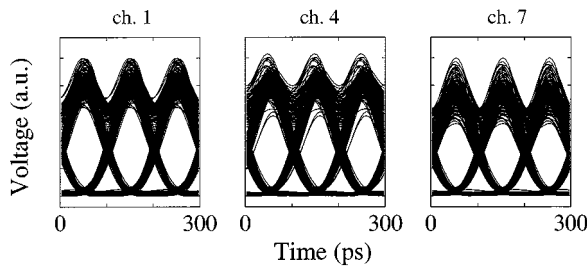


Fig. 20. Electrical eye diagrams of the CRZ seven-channel WDM system using LEAF fiber.

still dominated by the dispersion; the noise accumulation is still dominated by amplitude jitter due to signal-spontaneous beat noise; the nonlinearity still implies that symmetric compensation yields better eye diagrams than asymmetric compensation. The simulations with LEAF fiber show that there are significant advantages to reducing the nonlinearity while keeping the signal power the same. We conclude that nonlinearity plays an important role in CRZ systems, and its effect is always deleterious with this pulse modulation format.

## VI. CONCLUSION

In this paper, we studied WDM systems with single-channel data transmission rates of 10 Gb/s. We began by comparing three different modulation formats: NRZ; RZ without initial chirp; and CRZ. We found that, in order to obtain a transmission distance greater than 5000 km with reasonable power margins, we had to use the CRZ modulation format. The remainder of our studies were based on this modulation format. Next, we studied the evolution of individual CRZ pulses. We found that their evolution is dominated by the chromatic dispersion and is only slightly affected by the nonlinearity at optimal power levels. Studying trains of pulses, we found that the spread in the eye diagrams was primarily due to amplitude jitter generated by spontaneous-signal beat noise—a signature of linear systems. At the same time, we found that it was important to use symmetric dispersion compensation rather than asymmetric compensation to minimize the effects of the nonlinearity. Likewise, we found that interchannel nonlinearities lead to additional spreading of the eye diagrams, although they do not alter the CRZ pulse dynamics.

Because the dynamics of the CRZ system is primarily linear, and because nonlinearity plays an important role in both design of the dispersion maps and in limiting the channel spacing, we believe that it is appropriate to refer to these systems as quasi-linear. This term captures the reality that these systems evolve like linear systems, but the pulse modulation format, the dispersion map, and the channel spacing are all chosen to reduce the impact of nonlinearity to an acceptable level.

## REFERENCES

- [1] C. A. Brackett, "Dense wavelength division multiplexing networks: Principles and applications," *IEEE J. Select. Areas Commun.*, vol. 8, pp. 948–964, Aug. 1990.
- [2] N. S. Bergano, C. R. Davidson, M. Ma, A. N. Pilipetskii, S. G. Evangelides, H. D. Kidorf, J. M. Darcie, E. A. Golovchenko, K. Rottwitz, P. C. Corbett, R. Menges, M. A. Mills, B. Pedersen, D. Peckham, A. A. Abramov, and A. M. Vengsarkar, "320 Gb/s WDM transmission (64 × 5 Gb/s) over 7,200 km using large mode fiber spans and chirped return-to-zero signals," in *Proc. OFC'98*, San Jose, CA, Feb. 1998, PD12.
- [3] F. Favre, D. L. Guen, and T. Georges, "20 Gbit/s soliton transmission over 5200 km of nonzero-dispersion-shifted fiber with 106 km dispersion-compensated span," *Electron. Lett.*, vol. 34, pp. 201–202, Jan. 22, 1998.
- [4] N. S. Bergano, C. R. Davidson, C. J. Chen, B. Pedersen, M. A. Mills, N. Ramanujam, A. B. Kidorf, H. D. Puc, M. D. Levonas, and H. Abdelkader, "640 Gb/s transmission of sixty-four 10 Gb/s WDM channels over 7,200 km with 0.33 (bits/s)/Hz spectral efficiency," in *Proc. OFC'99*, San Diego, CA, Feb. 1999, PD2.
- [5] T. Yu, E. A. Golovchenko, A. N. Pilipetskii, and C. R. Menyuk, "Dispersion-managed soliton interactions in optical fibers," *Opt. Lett.*, vol. 22, no. 11, pp. 723–725, 1997.
- [6] N. J. Smith, F. M. Knox, N. J. Doran, K. J. Blow, and I. Bennion, "Enhanced power solitons in optical fibers with periodic dispersion management," *Electron. Lett.*, pp. 54–55, Oct. 24, 1996.
- [7] R.-M. Mu, V. S. Grigoryan, C. R. Menyuk, G. M. Carter, and J. M. Jacob, "Comparison of theory and experiment for dispersion-managed solitons in a recirculating fiber loop," *IEEE J. Select. Topics Quantum Electron.*, vol. 6, pp. 248–257, Mar./Apr. 2000.
- [8] D. Marcuse, "Derivation of analytical expressions for the bit-error probability in lightwave systems with optical amplifiers," *J. Lightwave Technol.*, vol. 8, pp. 1816–1823, Dec. 1990.
- [9] T. Saito, N. Henmi, S. Fujita, M. Yamaguchi, and M. Shikada, "Prechirp technique for dispersion compensation for a high-speed long span transmission," *IEEE Photon. Technol. Lett.*, vol. 3, pp. 74–76, Jan. 1991.
- [10] N. S. Bergano, C. R. Davidson, and F. Heismann, "Bit-synchronous polarization and phase modulation scheme for improving the performance of optical amplifier transmission systems," *Electron. Lett.*, vol. 32, pp. 52–54, Jan. 4, 1996.
- [11] N. S. Bergano and C. R. Davidson, "Wavelength division multiplexing in long-haul transmission system," *J. Lightwave Technol.*, vol. 14, pp. 1299–1308, June 1996.
- [12] Y. Kodama and S. Wabnitz, "Compensation of NRZ signal distortion by initial frequency shifting," *Electron. Lett.*, vol. 31, pp. 1761–1762, Sept. 28, 1995.
- [13] S. Bigo, E. Desurvire, and O. Andouin, "Dual-control nonlinear-optical loop mirrors for all-optical soliton synchronous modulation," *Opt. Lett.*, vol. 21, no. 18, pp. 1463–1465, 1996.
- [14] I. Morita, M. Suzuki, N. Edagawa, K. Tanaka, S. Yamamoto, and S. Akiba, "Performance improvement by initial phase modulation in 20 Gbit/s soliton-based RZ transmission with periodic dispersion compensation," *Electron. Lett.*, vol. 33, pp. 1021–1022, June 5, 1997.
- [15] Y. Kodama, S. Kumar, and A. Maruta, "Chirped nonlinear pulse propagation in a dispersion-compensated system," *Opt. Lett.*, vol. 22, no. 22, pp. 1689–1691, 1997.
- [16] L. Ding, E. A. Golovchenko, A. N. Pilipetskii, C. R. Menyuk, and P. K. Wai, "Modulated NRZ signal transmission in dispersion maps," in *System Technologies*, ser. OSA Trends in Optics and Photonics, A. E. Willner and C. R. Menyuk, Eds. Washington, DC: Opt. Soc. Amer., 1997, vol. 12, pp. 204–206.
- [17] F. Favre, D. L. Guen, and T. Georges, "Experimental evidence of pseudo-periodical soliton propagation in dispersion-managed link," *Electron. Lett.*, vol. 34, pp. 1868–1869, Sept. 17, 1998.
- [18] J. P. Gordon and H. A. Haus, "Random walk of coherently amplified solitons in optical fiber transmission," *Opt. Lett.*, vol. 11, pp. 665–667, 1986.
- [19] L. F. Mollenauer, J. P. Gordon, and S. G. Evangelides, "The sliding-frequency guiding filter: An improved form of soliton jitter control," *Opt. Lett.*, vol. 17, no. 22, pp. 1575–1577, 1992.
- [20] J. M. Jacob and G. M. Carter, "Error-free transmission of dispersion-managed solitons at 10 Gbit/s over 24 500 km without frequency sliding," *Electron. Lett.*, vol. 33, pp. 1128–1129, June 19, 1997.
- [21] G. P. Agrawal, *Nonlinear Fiber Optics*, 2nd ed. London, U.K.: Academic, 1995.
- [22] P. V. Mamyshev and N. A. Mamysheva, "Pulse-overlapped dispersion-managed data transmission and intra-channel four-wave mixing," *Opt. Lett.*, vol. 24, no. 21, pp. 1454–1456, 1999.
- [23] M. J. Ablowitz and T. Hirooka, "Resonant nonlinear intra-channel interactions in strongly dispersion-managed transmission systems," *Opt. Lett.*, vol. 25, no. 24, pp. 150–1752, 2000.

- [24] W. H. Loh, R. I. Laming, A. D. Ellis, and D. Atkinson, "10 Gb/s transmission over 700 km of standard single-mode fiber with 10-cm chirped fiber grating compensator and duobinary transmitter," *IEEE Photon. Technol. Lett.*, vol. 8, pp. 1258–1260, Sept. 1996.
- [25] L. Corral, J. Marti, J. M. Fuster, and R. I. Laming, "True time-delay scheme for feeding optically controlled phase-array antennas using chirped-fiber gratings," *IEEE Photon. Technol. Lett.*, vol. 9, pp. 1529–1531, Nov. 1997.
- [26] E. Yamada, T. Imai, T. Komukai, and M. Nakazawa, "10 Gbit/s soliton transmission over 2900 km using 1.3  $\mu\text{m}$  singlemode fibers and dispersion compensation using chirped fiber Bragg gratings," *Electron. Lett.*, vol. 35, pp. 728–729, Sept. 1999.
- [27] S. Watanabe, T. Naito, and T. Chikama, "Compensation of chromatic dispersion in a single-mode fiber by optical phase conjugation," *IEEE Photon. Technol. Lett.*, vol. 5, pp. 92–95, Jan. 1993.
- [28] M. I. Hayee and A. E. Willner, "Pre- and post-compensation of dispersion and nonlinearities in 10-Gb/s WDM systems," *IEEE Photon. Technol. Lett.*, vol. 9, pp. 1271–1273, Sept. 1997.
- [29] A. Hasegawa and Y. Kodama, *Solitons in Optical Communications*. Oxford, U.K.: Clarendon, 1995, ch. 9.
- [30] R.-M. Mu and C. R. Menyuk, "Symmetric slope compensation in a long haul WDM system using the CRZ format," *IEEE Photon. Technol. Lett.*, vol. 13, pp. 797–799, Aug. 2001.
- [31] T. Yu, W. M. Reimer, V. S. Grigoryan, and C. R. Menyuk, "A mean field approach to WDM simulations," *IEEE Photon. Technol. Lett.*, vol. 12, pp. 443–445, Apr. 2000.
- [32] Y. Sun, J. B. Judkins, A. K. Srivastava, L. Garret, J. L. Zyskind, J. W. Sulhoff, C. R. Wolf, M. Derosier, A. H. Gnauck, R. W. Tkach, J. Zhou, R. P. Espindola, A. M. Vengsarkar, and A. R. Vengsarkar, "Transmission of 32-WDM 10-Gb/s channel over 640 km using broad-band, gain-flattened Erbium-doped silica fiber amplifiers," *IEEE Photon. Technol. Lett.*, vol. 9, pp. 1652–1654, Dec. 1996.

**R.-M. Mu**, photograph and biography not available at the time of publication.

**T. Yu**, photograph and biography not available at the time of publication.

**V. S. Grigoryan**, photograph and biography not available at the time of publication.



**C. R. Menyuk** (SM'88–F'98) was born March 26, 1954. He received the B.S. and M.S. degrees from the Massachusetts Institute of Technology, Cambridge, in 1976 and the Ph.D. degree from the University of California, Los Angeles, in 1981.

He has worked as a Research Associate at the University of Maryland, College Park, and at Science Applications International Corporation, McLean, VA. In 1986, he became an Associate Professor in the Department of Electrical Engineering at the University of Maryland Baltimore County (UMBC), Baltimore, and he was the founding member of this department. In 1993, he was promoted to Professor. He has been on partial leave from UMBC since 1996. From 1996 to 2001, he worked part-time for the Department of Defense (DoD), codirecting the Optical Networking Program at the DoD Laboratory for Telecommunications Sciences, Adelphi, MD, from 1999 to 2001. In August, 2001, he left the DoD and became Chief Scientist at PhotonEx Corporation, Maynard, MA. For the last 15 years, his primary research area has been theoretical and computational studies of fiber-optic communications. He has authored or coauthored more than 140 archival journal publications as well as numerous other publications and presentations. He has also edited two books. The equations and algorithms that he and his research group at UMBC have developed to model optical fiber transmission systems are used extensively in the telecommunications industry.

Dr. Menyuk is a Fellow of the Optical Society of America (OSA) and a member of the Society for Industrial and Applied Mathematics and the American Physical Society. He is a former UMBC Presidential Research Professor.